Inorganic Chemistry
Article

Inorg. Chem. **2009**, *48*, 11123–11130 **11123**
DOI: 10.1021/ic9015004

Theoretical Study of Structure and Electronic Absorption Spectra of Some Schiff Bases and Their Zinc Complexes

Kseniya G. Vladimirova,*,†,‡ Alexandra Ya. Freidzon,† Oxana V. Kotova,‡ Andrei A. Vaschenko,§ Leonid S. Lepnev,§ Alexander A. Bagatur'yants,† Alexei G. Vitukhnovskiy,§ Nickolai F. Stepanov,‡ and Michael V. Alfimov†

†*Photochemistry Center, Russian Academy of Sciences, ul. Novatorov 7a, 117421 Moscow, Russia,* ‡*Department of Chemistry, Lomonosov Moscow State University, Leninskie gory 1/3, Moscow, 119991 Russia, and* §*Lebedev Physical Institute, Russian Academy of Sciences, Leninskii pr. 53, Moscow, 119991 Russia*

Received July 29, 2009

Tetradentate Schiff bases (H_2L^i), derivatives of salicylic aldehyde (H_2L^1, H_2L^2) or *o*-vanillin (H_2L^3, H_2L^4) with ethylenediamine or *o*-phenylenediamine as a bridge, and their zinc complexes were studied experimentally and theoretically in view of their possible application as emitters in organic light emitting diodes (OLEDs). The composition of thin films of the complexes was analyzed using a combination of different experimental and molecular modeling techniques taking into account changes in the Gibbs free energy of dehydration and dimerization reactions. The absorption spectra of the initial Schiff bases were investigated in methanol solutions, while the absorption spectra of their zinc complexes were investigated in thin films. Experimental results of elemental analysis, IR spectroscopy, laser desorption/ionization mass spectrometry (LDI MS), and X-ray diffraction as well as theoretical analysis of electronic absorption spectra by the quantum-chemical TD DFT method demonstrate that thin films of the zinc complexes contain binuclear anhydrous molecules. This conclusion should be taken into account when considering both transport and luminescence properties of these complexes in OLED heterostructures. A comparison of the results of CIS, TD DFT/PBE, and TD DFT/PBE0 calculations reveals the crucial importance of the inclusion of the exact exchange in the E_{XC} functional for the further correct description of potential energy surfaces of excited states for the systems studied.

Introduction

Zinc complexes with salen ligands (salen = *N*,*N*′-ethylenebis(salycilidenediamine)) can be used as sensing materials for different ions and molecules,[1] emissive materials for organic light emitting diodes (OLEDs),[2] building blocks for various supramolecular architectures,[3] etc. The spectra of Zn(salen) complexes depend on the substituents in the organic ligand and on the type of the coordination center.[2−6] The structure and spectral properties of these compounds and their dependence on the above factors can be predicted by quantum chemical simulation. At the same time, these calculations can provide better understanding of the experimental data on the optical properties of the compounds.[7]

Density functional theory (DFT) is an efficient and cost-effective tool for studying the structure of metal complexes with organic ligands. For example, in ref 8 the geometric parameters, dipole moments, and dissociation energies were calculated for a series of zinc coordination compounds ($Zn(H_2O)_2^{2+}$, $Zn(NH_3)_2^{2+}$, $Zn(NH_3)_2(OH)_2$, etc.) using various DFT-based methods in a nonrelativistic approximation and quasi-relativistic multielectron-fit pseudopotentials (MEFIT). The authors compared the results obtained using a wide variety of functionals with the results of coupled-cluster

*To whom correspondence should be addressed. E-mail: kgvladi@gmail.com.

(1) (a) Cano, M.; Rodríguez, L.; Lima, J. C.; Pina, F.; Dalla Cort, A.; Pasquini, Ch.; Schiffanio, L. *Inorg. Chem.* **2009**, *48*(13), 6229. (b) German, M. E.; Vargo, T. R.; McClure, B. A.; Rack, J. J.; Van Pattern, P. G.; Odoi, M.; Knapp, M. J. *Inorg. Chem.* **2008**, *47*, 6203. (c) Germain, M. E.; Vargo, T. R.; Khalifah, P. G.; Knapp, M. J. *Inorg. Chem.* **2007**, *46*, 4422.

(2) Müllen, K.; Scherf, U. *Organic Light Emitting Devices: Synthesis, Properties and Application*; Wiley-VCH, 2006.

(3) (a) Liu, X.; Hu, Y.-S.; Müller, J.-O.; Schlögl, R.; Maier, J.; Su, D. S. *Angew. Chem., Int. Ed.* **2009**, *48*, 210. (b) Wezenberg, S. J.; Kleij, A. W. *Angew. Chem., Int. Ed.* **2008**, *47*, 2354. (c) Kleij, A. W. *Dalton Trans.* **2009**, *24*, 4635.

(4) Yu, G.; Yin, S.; Liu, Y.; Shuai, Z.; Zhu, D. *J. Am. Chem. Soc.* **2003**, *125*, 14816.

(5) Yu, G.; Liu, Y.; Song, Y.; Wu, X.; Zhu, D. *Synth. Met.* **2001**, *117*, 211.

(6) (a) Cozzi, P. G.; Dolci, L. S.; Garelli, A.; Montalti, M.; Prodi, L.; Zaccheroni, N. *New J. Chem.* **2003**, *27*, 692. (b) Gradinaru, J.; Forni, A.; Druta, V.; Tessore, F.; Zecchin, S.; Quici, S.; Garbalau, N. *Inorg. Chem.* **2007**, *46*, 884.

(7) (a) Ohshima, A.; Momotake, A.; Arai, T. *J. Photochem. Photobiol. A* **2004**, *162*, 473. (b) Filarowski, A.; Koll, A.; Karpfen, A.; Wolschann, P. *Chem. Phys.* **2004**, *297*, 323. (c) Arslana, H.; Algülb, Ö.; Önkol, T. *Spectrochim. Acta Part A* **2008**, *71*, 191. (d) Yuan, Z.-L.; Zhang, Q.-L.; Liang, X.; Zhu, B.-X.; Lindoy, L. F.; Wei, G. *Polyhedron* **2008**, *27*, 344. (e) Yu, T.; Zhang, K.; Zhao, Y.; Yang, C.; Zhang, H.; Qian, L.; Fan, D.; Dong, W.; Chen, L.; Qiu, Y. *Inorg. Chim. Acta* **2008**, *361*, 233. (f) Fuentealba, M.; Garland, M. T.; Carrillo, D.; Manzur, C.; Hamon, J.-R.; Saillard, J.-Y. *Dalton Trans.* **2008**, 77. (g) Lacroix, P. G.; Bella, S. Di; Ledoux, I. *Chem. Mater.* **1996**, *8*, 541. (h) Ganjali, M. R.; Norouzi, P.; Faridbod, F.; Ghorbani, M.; Adib, M. *Anal. Chim. Acta* **2006**, *569*, 35.

(8) Dolg, M.; Wedig, U.; Stoll, H.; Preuss, H. *J. Chem. Phys.* **1987**, *86*, 866.

Published on Web 11/05/2009

calculations with single and double excitations and noniterative triples corrections (CCSD(T)) and with the results of semiempirical methods. The authors showed that hybrid exchange-correlation functionals, in particular, PBE0 and B3LYP, provide a satisfactory agreement with CCSD(T) results both for the dissociation energies and the geometry of the complexes. Taking relativistic effects into account results in longer Zn−L bond lengths and slightly changes the dissociation energies.

The introduction of different substituents in the ligand provides a way of tuning the optical properties of these compounds.[6,9−11] According to the Kasha rule,[12] the emission occurs from the lowest singlet excited state. Therefore, a correct description of emitting species and the nature and energy of the lowest singlet excited state is of crucial importance. Conventional methods used to describe spectral properties of large molecules include configuration interaction singles method (CIS)[13−15] and time-dependent density functional theory (TD DFT).[16,17] For some types of excitations (charge-transfer (CT) and Rydberg states), the TD DFT results depend on the nonlocal behavior of the chosen exchange-correlation functional.[17−21]Thus, large errors can occur in CT excitations because the spatial overlap between the orbitals participating in the transition is small.[22] One of the goals of this paper is to elucidate the importance of the inclusion of the exact exchange in the E_{XC} functional by simulating the absorption spectra of these molecules using various quantum-chemical methods.

It is known that the studied zinc complexes (Scheme 1) can be crystallized as mononuclear monohydrates $ZnL^i \cdot H_2O$[23] or binuclear anhydrous $[ZnL^i]_2$[24] molecules. However, the conventional synthetic procedure,[25] namely, the reaction of zinc acetate dihydrate ($Zn(CH_3COO)_2 \cdot 2H_2O$) with the corresponding Schiff base in ethanol at room temperature, produces $ZnL^i \cdot H_2O$ complexes with high yield. The (1:1) composition of the hydrated zinc complexes with Schiff base ligands was studied in detail in our previous work[9] using a combination of elemental, IR spectroscopy, thermal analysis under nitrogen atmosphere, and X-ray powder diffraction analysis of the complexes in combination with single crystal X-ray diffraction data. It is these complexes that were used as precursors for the deposition of emissive layers to construct new prototype OLEDs by thermal evaporation method ($p \sim 10^{-5}$ mbar).[26] The composition and physicochemical properties of the layers have an immediate effect on the characteristics of OLEDs. However, it is difficult to characterize the composition of these complexes in films, since these films are rather thin (~60−100 nm).

Scheme 1. Schematic structures of the Schiff bases (H_2L^i) and Zn-complexes (ZnL^i)

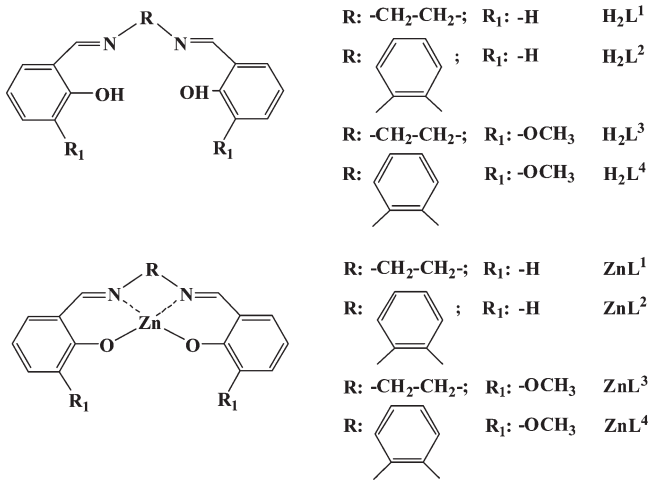

The experimental X-ray diffraction data of $ZnL^1 \cdot H_2O$ and $[ZnL^1]_2$ monocrystals indicate only minor structural changes occur in the monomeric unit when going from the hydrated mononuclear complex to the binuclear one. Therefore, one could expect that thermal evaporation used to prepare thin films should result in the dehydration of the $ZnL^i \cdot H_2O$ complexes, $ZnL^i \cdot H_2O \rightarrow ZnL^i + H_2O$ (1), followed by the dimerization of the anhydrous molecules, $2\ ZnL^i \rightarrow [ZnL^i]_2$ (2). To verify this suggestion, we investigated the composition of the deposited thin films using a combination of different experimental techniques and molecular modeling approaches. Since the evaporation process takes place in vacuum at a rather high temperature, we considered only a gas-phase reaction. Experimentally, we characterized the composition of the initial and evaporated zinc complexes using elemental analysis, IR spectroscopy, laser desorption/ionization mass spectrometry (LDI-MS), and X-ray diffraction. Theoretically, we simulated the changes in the Gibbs free energy in the dehydration and dimerization reactions in vacuum and the absorption spectra of monohydrate ($ZnL^i \cdot H_2O$) and binuclear ($[ZnL^i]_2$) forms of zinc complexes by TD DFT. The TD

(9) Kotova, O. V.; Eliseeva, S. V.; Averyushkin, A. S.; Lepnev, L. S.; Vaschenko, A. A.; Rogachev, A.Yu.; Vituhnovskii, A. G.; Kuz'mina, N. P. *Russ. Chem. Bull.* **2008**, *9*, 1880.
(10) Lo, W.-K.; Wong, W.-K.; Wong, W.-Y.; Guo, J.; Yeung, K.-T.; Cheng, Y.-K.; Yang, X.; Jones, R. A. *Inorg. Chem.* **2006**, *45*, 9315.
(11) Garnovskii, A. D.; Vasilchenko, I. S.; Garnovskii, D. A.; Kharisov, B. I. *J. Coord. Chem.* **2009**, *62*(2), 151.
(12) Kasha, M. *Farad. Disc.* **1950**, *9*, 14.
(13) (a) Levine, B. G.; Martínez, T. J. *Annu. Rev. Phys. Chem.* **2007**, *58*, 613. (b) Martknez, T. J. *Acc. Chem. Res.* **2006**, *39*, 119.
(14) Shukla, M. K.; Mishra, S. K.; Kumar, A.; Mishra, P. C. *J. Comput. Chem.* **2000**, *21*(10), 826.
(15) (a) Broo, A.; Lincoln, P. *Inorg. Chem.* **1997**, *36*, 2544. (b) Broo, A.; Holmén, A. *J. Chem. Phys.* **1997**, *101*, 3589.
(16) (a) Stratmann, R. E.; Scuseria, G. E.; Frisch, M. J. *J. Chem. Phys.* **1998**, *109*, 8218. (b) Bauernschmitt, R.; Ahlrichs, R. *Chem. Phys. Lett.* **1996**, *256*, 454. (c) Casida, M. E.; Jamorski, C.; Casida, K. C.; Salahub, D. R. *J. Chem. Phys.* **1998**, *108*, 4439.
(17) Head-Gordon, M.; Dreuw, A. *Chem. Rev.* **2005**, *105*, 4009.
(18) Dreuw, A.; Fleming, G. R.; Head-Gordon, M. *Phys. Chem. Chem. Phys.* **2003**, *5*, 3247.
(19) Tozer, D. J.; Amos, R. D.; Handy, N. C.; Roos, B. J.; Serrano-Andres, L. *Mol. Phys.* **1999**, *97*, 859.
(20) Dreuw, A.; Head-Gordon, M. *J. Am. Chem. Soc.* **2004**, *126*, 4007.
(21) Dunietz, B. D.; Dreuw, A.; Head-Gordon, M. *J. Phys. Chem. B* **2003**, *107*, 5623.
(22) Peach, M. J. G.; Benfield, P.; Helgaker, T.; Tozer, D. J. *J. Chem. Phys.* **2008**, *128*, 044118.
(23) Hall, D.; Moore, F. H. *J. Chem. Soc.* **1966**, (*A*), 1822.
(24) (a) Odoko, M.; Tsuchida, N.; Okabe, N. *Acta Crystallogr.* **2006**, *E62*, m708. (b) Mizukami, S.; Houjou, H.; Nagawa, Y.; Kanesato, M. *Chem. Commun.* **2003**, 1148. (c) Mizukami, S.; Houjou, H.; Sugaya, K.; Koyama, E.; Tokuhisa, H.; Sasaki, T.; Kanesato, M. *Chem. Mater.* **2005**, 50. (d) Singer, A. L.; Atwood, D. A. *Inorg. Chim. Acta* **1998**, *277*, 157. (e) Reglinski, J.; Morris, S.; Stevenson, D. E. *Polyhedron* **2002**, *21*, 2175. (f) Szłyk, E.; Wojtczak, A.; Surdykowski, A.; Goździkiewicz, M. *Inorg. Chim. Acta* **2005**, *358*, 467. (g) Wezenberg, S. L.; Escudero-Adán, E. C.; Benet-Buchholz, J.; Kleij, A. W. *Inorg. Chem.* **2008**, *47*, 2925. (h) Kleij, A. W. *Chem.—Eur. J.* **2008**, *14*, 10520. (i) San Felices, L.; Escudero-Adán, E. C.; Benet-Buchholz, J.; Kleij, A. W. *Inorg. Chem.* **2009**, *48*, 846.
(25) Batley, G. E.; Graddon, D. P. *Aust. J. Chem.* **1967**, *20*, 877.
(26) (a) Lepnev, L. S.; Vaschenko, A. A.; Vitukhnovsky, A. G.; Eliseeva, S. V.; Kotova, O. V.; Kuzmina, N. P. *Synth. Met.* **2009**, *158*, 625. (b) Lepnev, L. S.; Vaschenko, A. A.; Vitukhnovsky, A. G.; Eliseeva, S. V.; Kotova, O. V.; Kuzmina, N. P. *J. Russ. Laser Res.* **2008**, *29*(5), 497.

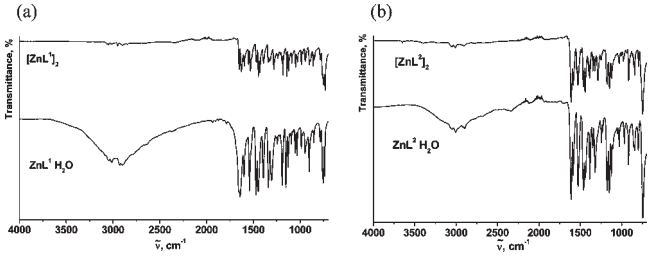

Figure 1. IR spectra of the initial complexes $ZnL^i \cdot H_2O$ and their sublimates ($[ZnL^i]_2$) ((a) – $i = 1$; (b) – $i = 2$).

DFT calculations were performed using the local gradient-corrected PBE,[27] hybrid B3LYP,[28] and PBE0[29] functionals with different basis sets. Calculations for the monohydrate ($ZnL^i \cdot H_2O$) zinc complexes and for the free ligands were also performed by the CIS method to elucidate the role of the exact exchange in the description of the excitation energy for different type transitions. The results were compared with the experimental absorption spectra of H_2L^i solutions and thin films of their zinc complexes.

Results and Discussion

Experimental Data. To characterize the composition of the complexes in thin films deposited by thermal evaporation in vacuum, we have analyzed the composition of the initial $ZnL^i \cdot H_2O$ complexes and their sublimates by elemental analysis, IR spectroscopy, LDI-MS, and X-ray powder diffraction. The results of elemental analysis of the sublimed samples correspond to anhydrous compounds. Their IR spectra, in contrast to hydrated complexes ($ZnL^i \cdot H_2O$), display no broad absorption band corresponding to vibrations of the water molecule at ~3500−2500 cm^{-1} (Figure 1). However, for both the initial and sublimed samples, the positions of the characteristic C−H, C═N, aromatic ring, and C−O vibrations remain almost the same, which indicates that the structures of these species are rather similar. The most intense signals in the LDI mass spectra (Table S1) of $ZnL^i \cdot H_2O$ dissolved in dimethyl formamide correspond to mononuclear ions $[ZnL^i + Na^+]^+$ or $[ZnL^i]^+$. However, binuclear ions have also been detected by LDI-MS.

Using the known data of X-ray diffraction analysis for both $ZnL^i \cdot H_2O$ and $[ZnL^i]_2$ ($i = 1, 2$) single crystals,[10−24] we simulated their theoretical XRD patterns to evaluate the composition of the sublimed samples (Figure S1). Hence, from the analysis of the experimental results, we can conclude that the anhydrous compounds consist of binuclear zinc complexes $[ZnL^i]_2$.

Molecular Simulation. The equilibrium geometries of the studied compounds are shown in Figure 2. The molecules of the Schiff bases are symmetric (C_2). The salicylidene moieties in H_2L^1 and H_2L^3 are parallel, while two salicylidene moieties and *o*-phenylene bridge in H_2L^2 and H_2L^4 together with adjacent nitrogen atoms form an angle $\alpha = 39°$. Nevertheless, the salicylidene moieties in H_2L^1 and H_2L^3 are not conjugated because of the aliphatic bridge between them, whereas two salicylidene moieties and the *o*-phenylene bridge in H_2L^2 and H_2L^4 form a common π-conjugated system.

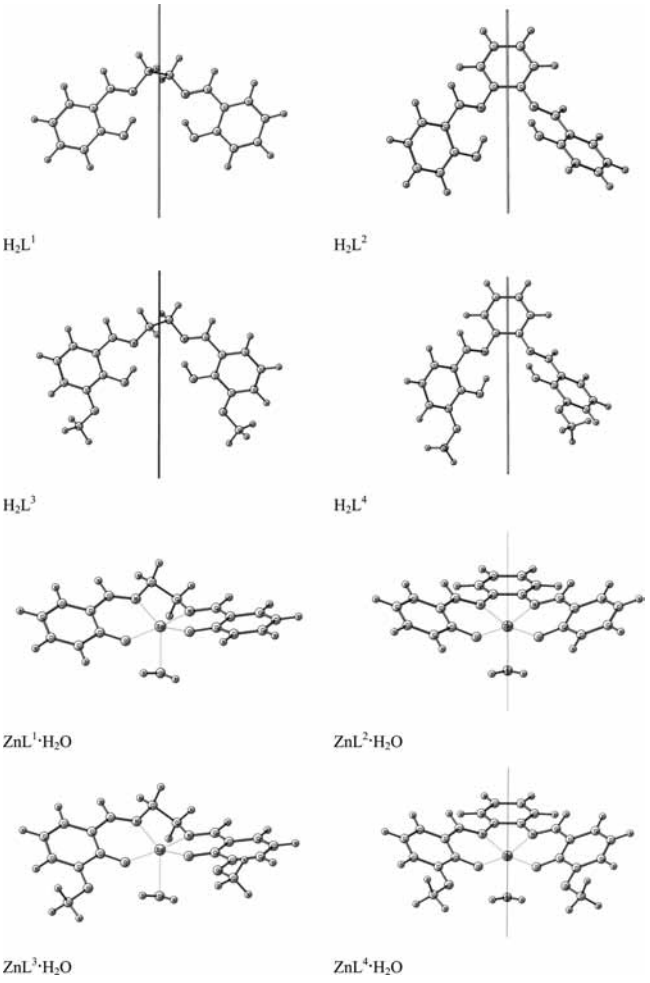

Figure 2. Equilibrium geometries of H_2L^i and $ZnL^i \cdot H_2O$. Lines indicate the 2-fold axis (for C_2 symmetric structure) and mirror planes (for C_s symmetric structure).

Both $ZnL^2 \cdot H_2O$ and $ZnL^4 \cdot H_2O$ molecules exhibit C_s symmetry. The mirror planes are perpendicular to the molecule plane and $C_{ar}-C_{ar}$ bond of the aromatic bridge. In contrast, $ZnL^1 \cdot H_2O$ and $ZnL^3 \cdot H_2O$ monohydrates are asymmetric. In this case, the complexation with zinc results in the rearrangement of the salicylidene moieties as compared to the initial Schiff bases. The donor O and N atoms of the Schiff base in $ZnL^1 \cdot H_2O$ and $ZnL^3 \cdot H_2O$ are located in different planes relative to each other, whereas in $ZnL^1 \cdot H_2O$ and $ZnL^3 \cdot H_2O$ they are coplanar. Obviously, the zinc complexes are more rigid than the structures of the ligands.

The calculated binuclear structures $[ZnL^i]_2$ are centrally symmetric (Figure 3). The M−L bond lengths satisfactorily agree with the X-ray diffraction data. Zn and O atoms of the salicylidene moieties form a planar tetragon (nearly square) with Zn−O distances ~2.1 Å, O−Zn−O and Zn−O−Zn angles ~83−86 and 97−94°, respectively. In projection to the rms (root-mean-square) planes of the ligands, the salicylidene moieties overlap, while the bridges are opposite to each other. This means

(27) Perdew, J. P.; Burke, K.; Ernzerhof, M. *Phys. Rev. Lett.* **1996**, *77*, 3865; Err. 1997, 78, 1396.
(28) (a) Becke, A. D. *J. Chem. Phys.* **1993**, *98*, 5648. (b) Stephens, P. J.; Devlin, F. J.; Chablowski, C. F.; Frisch, M. J. *J. Phys. Chem.* **1994**, *98*, 11623. (c) Hertwig, R. H.; Koch, W. *Chem. Phys. Lett.* **1997**, *268*, 345.
(29) (a) Ernzerhof, M.; Scuseria, G. E. *J. Chem. Phys.* **1999**, *110*, 5029. (b) Adamo, C.; Barone, V. *J. Chem. Phys.* **1999**, *110*, 6158.

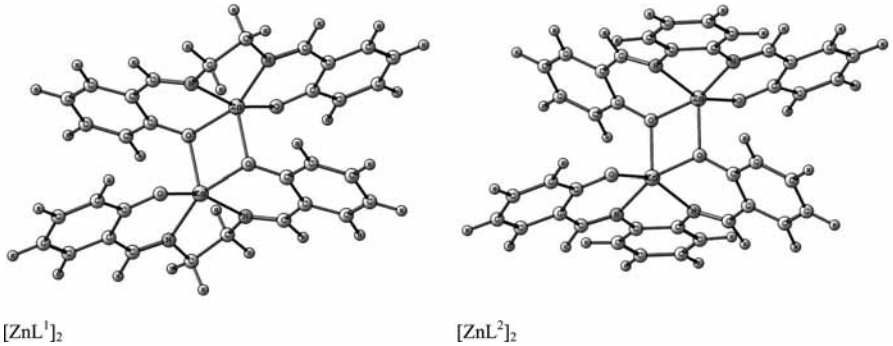

Figure 3. Equilibrium geometries of $[ZnL^1]_2$ and $[ZnL^2]_2$.

Table 1. Gibbs Free Energy of the Reaction 3 in Vacuum Calculated Using Partition Functions for Different Temperatures

T, K	$\Delta G^T(ZnL^1)$, kcal/mol	$\Delta G^T(ZnL^2)$, kcal/mol	$\Delta G^T(ZnL^3)$, kcal/mol	$\Delta G^T(ZnL^4)$, kcal/mol
298.15	−9.6	−9.6	−8.6	−9.5
373.15	−11.5	−11.5	−10.1	−11.2
473.15	−13.9	−14.0	−12.2	−13.6

that the molecular orbitals (MOs) of the salicylidene moieties interact, which will result in substantial spectral changes, as will be seen below.

The calculation of the thermodynamical parameters of dehydration (1) and dimerization (2) processes in vacuum demonstrates that the Gibbs energy of the cumulative reaction (3) is negative for all studied complexes and increases in absolute value with the temperature (Table 1).

$$2ZnL^i \cdot H_2O \rightarrow [ZnL^i]_2 + 2H_2O \qquad (3)$$

Thus, dehydration of $ZnL^i \cdot H_2O$ complexes followed by the dimerization into $[ZnL^i]_2$ in the course of their thermal evaporation and formation of thin films on the substrate is favorable. This is supported by the experimental data above.

Simulation of the Absorption Spectra. Adding an aromatic moiety ($H_2L^1 \rightarrow H_2L^2$, $H_2L^3 \rightarrow H_2L^4$) or a donor substituent ($H_2L^1 \rightarrow H_2L^3$, $H_2L^2 \rightarrow H_2L^4$) to the ligand results in the bathochromic shift of the absorption bands both in the short-wave and long-wave parts of the spectra (Table S2, Figure 4). The energies and intensities of the transitions calculated by the TD DFT method using the hybrid PBE0 functional qualitatively agree with the experimental absorption spectra and reproduce the regularities mentioned above, although not exactly. Solvation by a polar solvent can affect relative intensities of the bands so that the intensity of this transition changes in solution.

As noted in refs 14 and 15, the transition energies in CIS calculations are strongly overestimated, and it is necessary to scale them by a factor $k = 0.72$ to match the experimental data. As one can see from a comparison of the results of CIS, TD DFT/PBE, and TD DFT/PBE0 calculations (Table S2), many low-lying transitions with low intensities are observed for all systems with high dipole moments of excited states only in the TD DFT/PBE calculation. This means that an addition of the exact exchange in the E_{XC} functional is of crucial importance for the correct description of excitation energies for the systems studied.

The transition energies calculated by TD DFT with a hybrid functional PBE0 and different basis sets are close; the difference in the transition energies is ~0.02−0.07 eV (Table S3). Adding polarization *d* and *p* functions to the basis set only slightly changes the transition energy ($\Delta E \approx 0.05$) and its intensity ($\Delta f \approx 0.03$).

The intense transitions in the complexes in study are of $\pi \rightarrow \pi^*$ type. The analysis of the orbitals involved in the intense transitions showed that, in the Schiff bases with the aliphatic bridge H_2L^1 and H_2L^3, both **HOMO − 1** and **HOMO** and **LUMO** and **LUMO + 1** are a sum and a difference of the orbitals of the salicylidene moieties. As a result of the arrangement of the salicylidene moieties, the orbitals participating in the low-lying transitions in $ZnL^1 \cdot H_2O$ and $ZnL^3 \cdot H_2O$ are mainly localized on each salicylidene moiety, whereas in $ZnL^2 \cdot H_2O$ and $ZnL^4 \cdot H_2O$ they are delocalized over the entire π system of the molecule (Figure 6). In the case of $ZnL^1 \cdot H_2O$ and $ZnL^3 \cdot H_2O$, only the transitions localized within each salicylidene moiety are allowed.

As shown above, thermal evaporation of the hydrated zinc complexes results in the formation of thin films consisting of binuclear species $[ZnL^i]_2$. This should be taken into account in simulation of the absorption spectra of the films. Figure 5 shows the comparison of the calculated absorption spectra of the monohydrates and binuclear zinc complexes with H_2L^1 and H_2L^2 Schiff bases with the experiment.

The absorption spectra of $[ZnL^1]_2$ and $[ZnL^2]_2$ are shifted to the long wavelengths compared to the spectra of the corresponding monomers. This accounts for the larger broadening of the absorption band in the spectrum of ZnL^1 film and indirectly supports that the concentration of binuclear species in the ZnL^2 film is high.

Relationship between the Ligand Structure and HOMO−LUMO Gap. The positions of the highest occupied molecular orbital (**HOMO**) and the lowest unoccupied molecular orbital (**LUMO**) are important molecular parameters immediately associated with the electron and hole transport properties of the substance. The **HOMOs** of the studied compounds are mainly localized on the oxygen atoms (including those in the methoxy groups). On the other hand, the **LUMOs** are mainly localized on the nitrogen atoms of the salicylidene moieties. Therefore, adding an aromatic moiety to the structure (replacing the ethylenediamine bridge by *o*-phenylenediamine) slightly (by ~0.1 eV) decreases the **HOMO**

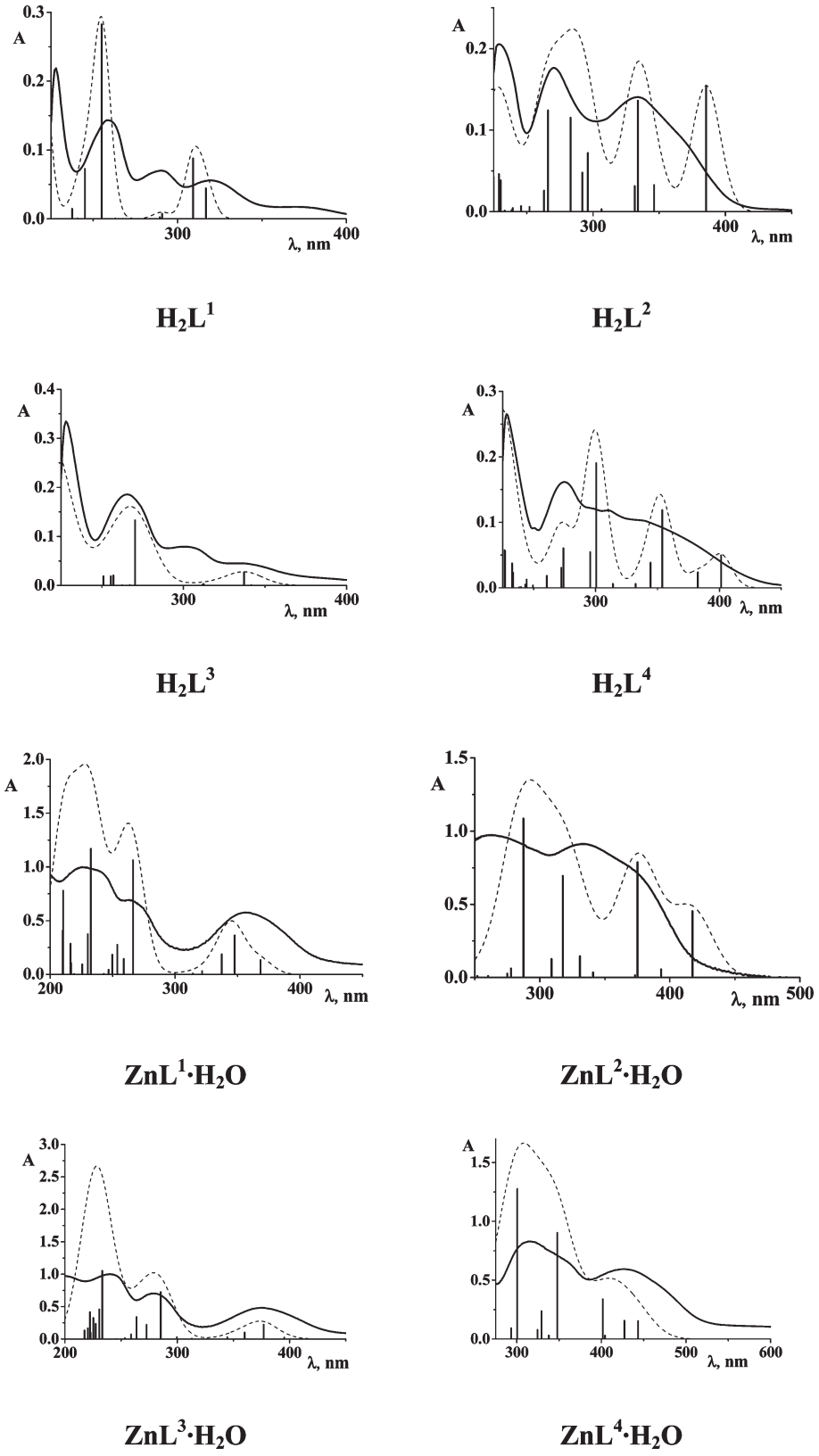

Figure 4. Experimental absorption spectra (solid lines) of H_2L^i (methanol solutions, $c = 10^{-5}$ M) and $ZnL^i \cdot H_2O$ (thin films with thickness of ~60−100 nm) and calculated ones (TD DFT, PBE0/TZV(d,p), vertical lines). The calculated spectra are broadened (dashed lines) and scaled to fit the experimental ones by a factor of 0.3 and 1.3 for the solution and film spectra, respectively.

energy and substantially (by 0.4−0.5 eV) decreases the **LUMO** energy and, therefore, decreases the energy gap by 0.6−0.7 eV in the Schiff bases and by ~0.3 eV in the complexes. At the same time, a donor substituent (methoxy group) has a greater effect on the **HOMO** energy (by 0.3−0.4 eV) than on the **LUMO** energy (by ~0.15 eV), but it also reduces the energy gap by ~0.2 eV. Hence, the energy gap in the compounds in study changes

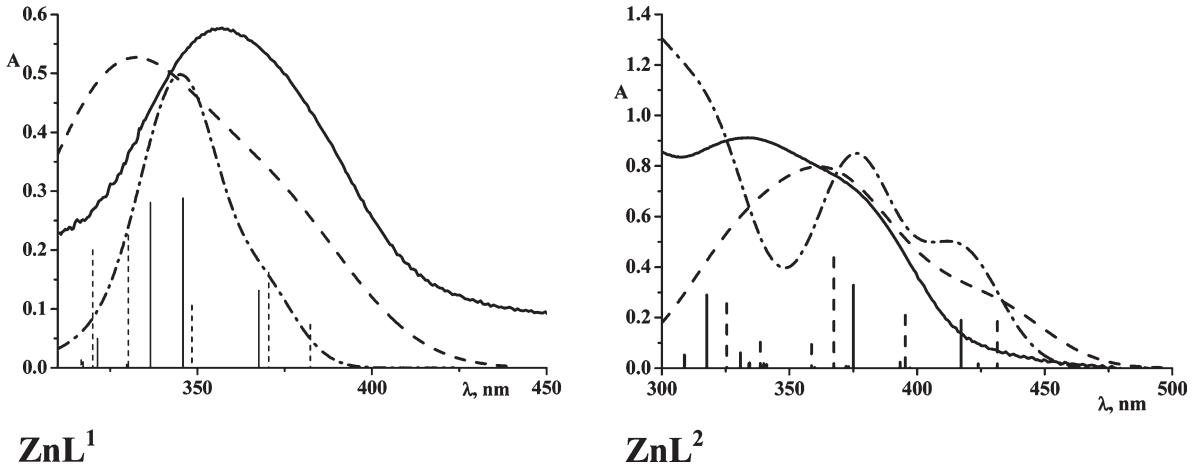

Figure 5. Long-wavelength (300−500 nm) part of the absorption spectra of $[ZnL^i]_2$ (dashed lines) and $ZnL^i \cdot H_2O$ (dash-dotted lines) ($i = 1, 2$) calculated by TD DFT, PBE0/TZV(d,p), (vertical dashed and solid lines, respectively) as compared to the experimental absorption spectra of the ~60−100-nm-thick films of zinc complexes (solid lines).

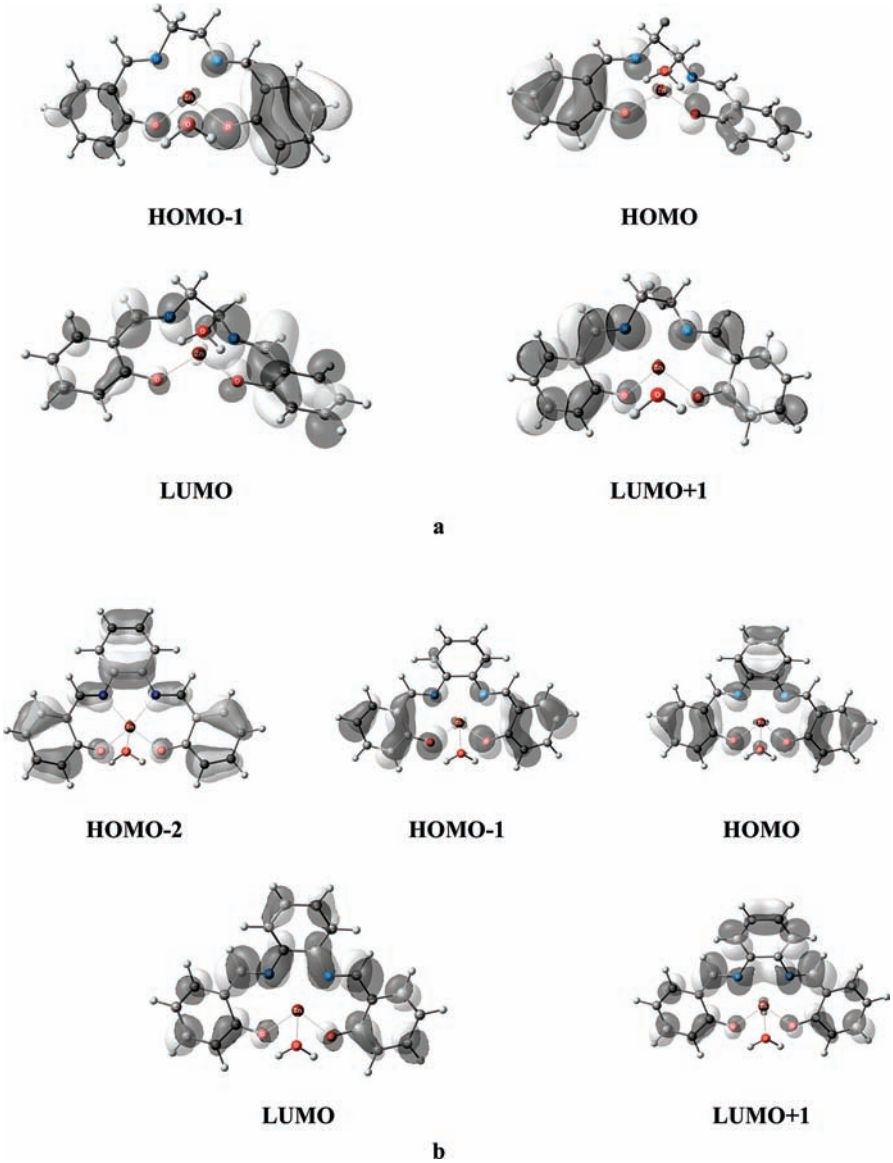

Figure 6. Molecular orbitals involved in the intense transitions of (a) $ZnL^1 \cdot H_2O$ and (b) $ZnL^2 \cdot H_2O$ from the DFT calculation (PBE0/TZV (d,p)).

in a following way:

$$\Delta E(H_2L^1/ZnL^1\cdot H_2O/[ZnL^1]_2) > \Delta E(H_2L^3/ZnL^3\cdot H_2O/[ZnL^3]_2) > \Delta E(H_2L^2/ZnL^2\cdot H_2O/[ZnL^2]_2) > \Delta E(H_2L^4/ZnL^4\cdot H_2O/[ZnL^4]_2)$$

Conclusions

The structure of zinc complexes with Schiff base ligands deposited in thin films was investigated using a combination of experimental and theoretical methods. It is demonstrated that the thermal evaporation of mononuclear $ZnL^i\cdot H_2O$ complexes results in the deposition of binuclear complexes $[ZnL^i]_2$, which form anhydrous thin films on the surface of the substrates. This fact is of great importance for the prediction of both the transport and luminescence properties of the zinc complexes in thin films.

It is shown that TD DFT calculations with the hybrid PBE0 functional qualitatively describe the positions and intensities of the absorption bands and reproduce the dependences observed in the absorption spectra upon variations of the ligand structure. However, a comparison of the results of CIS, TD DFT/PBE, and TD DFT/PBE0 calculations demonstrated that the inclusion of the exact exchange in the E_{XC} functional is of the crucial importance for the correct description of excitation energies in the systems studied. These conclusions should be taken into account in the further consideration of potential energy surfaces of excited states for the correct description of the emission spectra of zinc complexes.

Experimental Section

Characteristics of Zinc Complexes. $[ZnL^1]_2$ (bis-(*N*,*N*′-ethylene-bis(salycilidenediamine))zinc). Found (%): C 58.5, H 4.7, N 8.5. Calcd (%): C 57.9, H 4.2, N 8.5, $C_{32}H_{28}N_4O_4Zn_2$. IR (Diamond ATR): ν(C−H) 2898, 2846; υ(C=N) 1628, 1653; vibrations of aromatic ring 1436, 946, 860, 734; ν(C−O) 1184, 1130, 1125, 1090 cm^{-1}.

$[ZnL^2]_2$ ((*N*,*N*′-(*o*-phenylen)-bis(salycilidenediamine))zinc). Found (%): C 63.6, H 3.4, N 7.6. Calcd (%): C 63.3, H 3.7, N 7.4, $C_{40}H_{28}N_4O_4Zn_2$. IR (Diamond ATR): ν(C−H) 3076, 3009, 2904; υ(C=N) 1610; vibrations of aromatic ring 1442, 916, 844, 797, 746; ν(C−O) 1177, 1148, 1124 cm^{-1}.

Materials and Measurements. The Schiff bases (H_2L^i, i = 1−4) and corresponding zinc complexes ($ZnL^i\cdot H_2O$) were synthesized and characterized by elemental, IR, ^{1}H NMR, thermal and electron impact ionization mass spectrometry analyses, see ref 9.

Isothermal dynamic sublimation experiments were performed only with the $ZnL^1\cdot H_2O$ and $ZnL^2\cdot H_2O$ samples (~200 mg) placed in glass test tubes for about 30 min at 280−320 °C and a pressure of 10^{-2} Torr. Weight loss was equal to ~80%.

The composition of the sublimed samples was determined using the following experimental techniques.

Elemental analyses (C, H, N) were performed by the Microanalytical Service of the Center for Drug Chemistry (Moscow, Russia).

IR spectra were recorded in the range of 4000−600 cm^{-1} using a Perkin-Elmer Spectrum One spectrometer equipped with a universal attenuated total reflection sampler.

Direct laser desorption/ionization mass spectrometry (LDI MS) experiments of zinc complexes were performed with an Autoflex II (Bruker Daltonics, Germany) instrument. The spectra were recorded in positive mode using an accelerating voltage of 19 kV, whereas the desorption/ionization of the samples was achieved with nitrogen laser (337 nm, impulse of 1 ns). The typical procedure of sample preparation for LDI was applied.[30] Zinc complexes were dissolved in dimethyl formamide. The interpretation of the mass spectra was based on the general rules of fragmentation described for electron impact ionization mass spectrometry.[31]

XRD powder patterns (T = 293 K) for the initial hydrated and sublimed zinc complexes were collected using an Enraf-Nonius FR 552 Guinier Johansson camera equipped with a curved 111 quartz monocromator (Cu Kα, λ = 1.540598 Å).

Absorption spectra of the Schiff base solutions (c = 10^{-5} M, methanol) were recorded using an UV−vis Lambda 35 spectrophotometer (Perkin-Elmer) (spectral resolution 1 nm, optical path length l = 1 cm). The absorption spectra are corrected for the absorption of the solvent.

Thin films of zinc complexes were deposited on quartz substrates using thermal evaporation of $ZnL^i\cdot H_2O$ complexes with deposition rate ~1−3 Å/s in vacuum atmosphere (~10^{-5} mbar). The deposition temperature (140−200 °C) was lower than the temperature of the decomposition of the complexes (225−320 °C).[9] The film thickness and growth rate were monitored using a quartz crystal microbalance with an Inficon IC-6000 control unit. The thickness of the deposited films was in the range of ~60−100 nm. The absorption spectra of the thin films were recorded using an UV−vis SPECORD M40 spectrophotometer (Carl Zeiss Jena, Germany). The absorption spectra are corrected for the absorption of the silica substrates.

Molecular Modeling and Computational Details. X-ray diffraction data of H_2L^4,[10] $ZnL^1\cdot H_2O$,[23] and $[ZnL^1]_2$[24] were used for constructing the starting structures of the free ligands and complex monohydrates for geometry optimization. The calculations were performed using PRIRODA[32] and PCGAMESS/Firefly[33] program packages.

The geometry of the studied compounds was optimized by DFT using local PBE functional,[27] 3z basis set[32] of contracted Gaussian functions ((5s1p)/[3s1p] for H, (11s6p2d)/[6s3p2d] for C, O, and N, and (17s13p8d)/[12s9p4d] for Zn), and auxiliary density-fitting basis set of uncontracted Gaussian functions ((5s2p) for H, (10s3p3d1f) for C, N, and O, and (18s6p6d5f5g) for Zn).

The thermodynamic parameters of the complexes in study were calculated by PBE/3z in the "harmonic oscillator−rigid rotor" approximation for the partition function at different temperatures.

The transition energies and oscillator strengths were calculated by CIS and TD DFT methods. TD DFT calculations were performed using PBE,[28] B3LYP,[29] and PBE0[30] functionals with 6-31G(d,p) basis set and using PBE0 functional with TZV, 6-31G(d,p), and TZV(d,p) basis sets.

To compare the calculated absorption spectra with the experimental ones, we simulated the spectra through Doppler broadening of the calculated spectral lines taking into account their oscillator strengths:

$$I_D = I_0\cdot\exp[-((\nu-\nu_0)/\gamma)^2] \quad (4)$$

where $\gamma = (1/\sqrt{\ln 2})\cdot w_{1/2}$, and $w_{1/2}$ is the half width at the half height of the spectral band (ChemCraft v.1.6 program[34]). The

(30) Hunsucker, S. W.; Watson, R. C.; Tissue, B. M. *Rapid Commun. Mass Spectrom.* **2001**, *15*, 1334.
(31) Gerbeleu, N. V.; Indrichan, K. M. *Mass-Spectrometry of Coordination Compounds*; Shtiintca: Kishinev, **1984** (in Russian).
(32) Laikov, D. N. *Chem. Phys. Lett.* **1997**, *281*, 151.
(33) Granovsky, A. A.; *PC GAMESS version 7.1*. http://classic.chem.msu.su/gran/gamess/index.html.
(34) Zhurko, G.A.; *ChemCraft version 1.6*. http://www.chemcraftprog.com.

resulting curves were scaled to match the integral intensities of the calculated and experimental spectral bands.

Acknowledgment. This work was supported by the Russian Foundation for Basic Research (RFBR), grants 07-02-00495-a, 09-03-00850-a, 09-02-00546-a, and 09-03-00993-a, and by the Development Program for System of Leading Scientific Schools in Russia, grant NH-4365.2008.2. We are grateful to Prof. N. Kuzmina for useful discussions and for Mr. D. Tsymbarenko for his assistance in X-ray powder diffraction experiments.

Supporting Information Available: List of the main ion fragments of $ZnL^i \cdot H_2O$ (i = 1−4) and $[ZnL^i]_2$ (i = 1, 2), comparison of the energies and oscillator strengths of allowed transitions in $ZnL^i \cdot H_2O$ calculated by TD DFT with different functionals and by CIS/6-31G(d,p), transition energies of $ZnL^i \cdot H_2O$ calculated by TD DFT/PBE0 with different basis sets, XRD powder patterns of $ZnL^i \cdot H_2O$ and $[ZnL^i]_2$ (i = 1,2). This material is available free of charge via the Internet at http://pubs.acs.org.